November 2019

Indocyanine-Green-Assisted Near-Infrared Dental Fluorescence Imaging to Detect Common Dental Diseases, as Compared With Dental X-Ray

Yoshita Viraj Holamoge
Louisiana State University and Agricultural and Mechanical College

INDOCYANINE-GREEN-ASSISTED NEAR-INFRARED DENTAL FLUORESCENCE IMAGING TO DETECT COMMON DENTAL DISEASES, AS COMPARED WITH DENTAL X-RAY

A Thesis

Submitted to the Graduate Faculty of the
Louisiana State University and
Agricultural and Mechanical College
in partial fulfillment of the
requirements for the degree of
Master of Science

in

The Department of Electrical and Computer Engineering

by
Yoshita Viraj Holamoge
B.Tech., Manipal Institute of Technology, 2016
December 2019

ACKNOWLEDGEMENTS

I would like to sincerely thank my advisor Dr. Jian Xu for his support and guidance throughout my academic career as a master's student. His classes and teaching style inspired me in choosing biomedical imaging as my research area. I would also like to thank Dr. Shaomian Yao from the Department of Comparative Biomedical Sciences at the LSU School of Veterinary Medicine for his collaboration in this study. I would like to extend my gratitude to my thesis committee members, Dr. Guoxiang Gu and Dr. Jin-Woo Choi for their time as well as suggestions for improvement in my thesis.

I would also like to thank Mr. Zhongqiang Li (Ph.D. candidate) for his guidance and support during the experimentation phase of the study as well as the documentation. I would like to thank Mr. Zheng Li (Ph.D. candidate) for his guidance and assistance during the review of this thesis document. Their constructive inputs have greatly helped in compiling this document.

TABLE OF CONTENTS

LIST OF FIGURES

ABSTRACT

Oral health is indicative of a person's overall health. Even with advances in medical science, dental diseases are very much prevalent in our society. Dental imaging techniques help in the early detection of these dental diseases and eventually avoids the risk of poor oral health as well as medical expenses. Current dental imaging techniques rely mostly on X-ray imaging whose ionizing property is a concern amongst the population. Near-infrared spectrum is known to have tissue penetration property and they belong to the non-ionizing part of the electromagnetic spectrum. This study utilized a contrast agent assisted near-infrared imaging for common dental diseases. In specific, the advantages of using near-infrared window I (650nm-950nm) and near-infrared window II (950-nm -1700nm) with Indocyanine Green (ICG) as an imaging contrast agent in the detection of common dental diseases were explored and compared with X-ray dental imaging. ICG assisted near-infrared fluorescence (ICG-NIRF) imaging was successfully able to identify dental caries, dental decays as well as dental cracks. This study was able to detect enamel cracks which 3-D reconstructed X-ray failed to detect. ICG-NIRF provided enhanced contrast in the detection of enamel-dentin junction. It was observed that within a small immersion time a good contrast and fluorescence were seen using ICG-NIRF technique. Another major advantage of this method compared to the traditional radiographs is that it is a real time dental imaging technique. Lastly, the cost of the whole equipment is around $18,000 which is much lower than the 3-D X-ray equipment which is at least $100,000. This makes the equipment cost 5.5 times less than the currently used 3-D X-ray machines. Overall, this study has shown that ICG-NIRF provides good results in visualizing dental diseases and thus can be used as an alternative to X-ray imaging.

INTRODUCTION

Importance of Oral Health and Some Statistics on Common Dental Diseases

Oral health is a window to the overall health of the person. Poorly managed oral health can lead to difficulties in managing other systemic health related conditions. It could give rise to serious infections and in cases malnutrition as well. In elderly people it is also a factor that leads to poor self-esteem (Coleman, 2002). The World Health Organization defines oral health as "a state of being free from chronic mouth and facial pain, oral and throat cancer, oral infection and sores, periodontal (gum) disease, tooth decay, tooth loss, and other diseases and disorders that limit an individual's capacity in biting, chewing, smiling, speaking, and psychosocial wellbeing." (Petersen, 2003; WorldHealthOrganization, 2018). As estimated by the Global Burden of Disease Study 2016, dental diseases affect approx. 3.58 billion people across the world. One of the most common dental disease called caries, affects the permanent teeth of an astounding 2.4 billion people and the primary teeth of approx. 486 million children (Vos et al., 2017). According to National Health and Nutrition Exam Survey (NHANES), for the year 2015-2016, the prevalence of caries both treated and untreated in the youth group aged 2-19 was 45.8% (Fleming & Afful, 2018). Apart from caries, a leading cause for tooth loss is severe periodontal disease (Coleman, 2002). In 2016, it was estimated that severe periodontal disease, was the 11th most prevalent disease globally (Vos et al., 2017).

Cracked tooth, is another common dental disease. A statistical estimate shows that, cracked teeth is present in about 35% of the population (Hasan, Singh, & Salati, 2015). Cracked tooth can be define as the "incomplete fracture of the dentine in a vital posterior tooth that involves the dentine and occassionally extends to the pulp" (Bethany Cadman, 2018; Da Rosa, Pradebon, Brondani, Piva, & Da Silva, 2017). Cracked tooth can often lead to cracked tooth syndrome, which

is characterized by brief sharp pain in tooth, often not understood untill a piece fractures off (TÜRp & Gobetti, 1996) (Merskey, 1994). It is also one of the most difficult diseases to diagnose as it doesn't present defined symptoms (Banerji, Mehta, & Millar, 2010). This is a major cause for the often failed early disgnosis of cracked tooth. If untreated, tooth cracks can give rise to to bacterial infection and inflammation. (Rivera & Walton, 2008) With cracked tooth, the information of their location, direction as well as extent of crack are valuable information to the practitioners in designing the treatment plan (Rivera & Walton, 2008). According to the American Association of Endodontists (AAE) there are five types of dental cracks. They are craze lines, fractured cusp, cracked tooth, split tooth, and vertical root fracture (Da Rosa et al., 2017; Rivera & Walton, 2008). Figure 1 shows the four major types of cracked tooth excluding craze lines. The early stage benign cracks are called craze lines. Craze lines are mostly present in the enamel and can be found either in the occlusal, lingual or buccal region of the tooth (Mariona & Antony, 2018). It is a challenge for the clinicians to differentiate between the five types of cracks as they are not always clearly distingushable (Lubisich, Hilton, Ferracane, & Northwest, 2010).

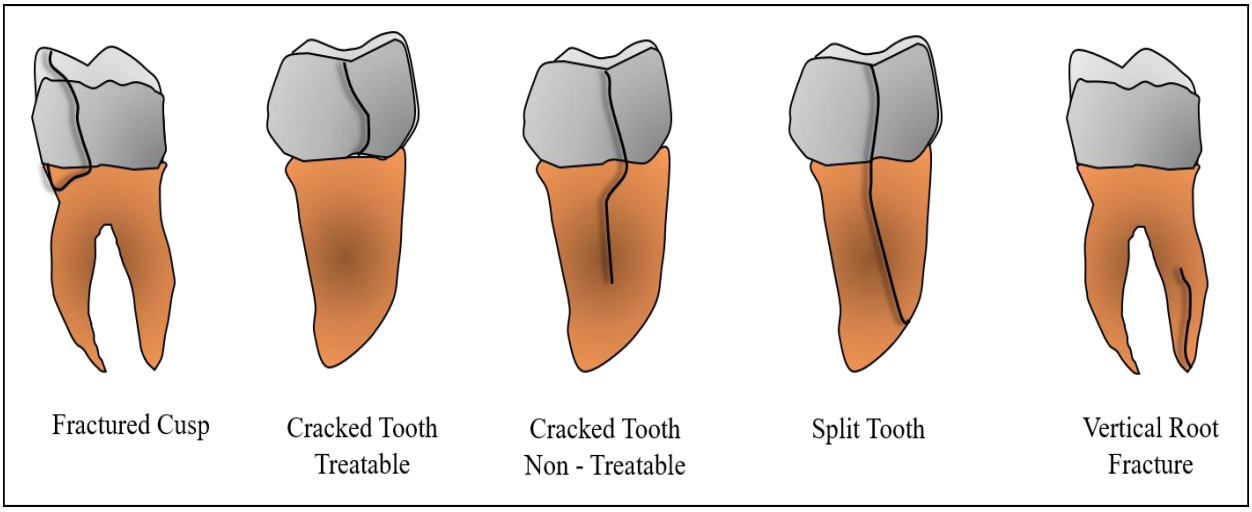

Figure 1. Types of Cracked Tooth

Today, the clinicians use the help of several techniques to diagonse cracked teeth. They usually begin with the anlysis of the dental history of the patient. This analysis helps the clinicians understand if the patient has bitten or chewed on a hard object, or if they have had previous dental treatments that could be the possible cause for the cracked tooth or its related symptoms. Tactile examination using a probe also called as the dental explorer can be used as a diagnostic method to detect cracks (Bethany Cadman, 2018; Mathew et al., 2012). Although, not the most efficient mode of diagnosing cracked tooth, visual examination aided by magnifying tools are also utilized by clinicians (Bethany Cadman, 2018). The clinicians awareness of dental cracks is a key factor in diagnosing cracked tooth and can prevent the progress of the crack into the tooth structure.(Mathew et al., 2012)

According to the World Health Organization, 5% of the total health expenditure is due to dental treatment as well as around 20% of the out of pocket expenditure (Blas & Kurup, 2010). In industrialized countries, oral health treatment is ranked the fourth most expensive treatment (Petersen, 2004). This makes dental treatment a costly affair. Also, socio – economic factors play an important role in people being able to afford quality dental treatment (Blas & Kurup, 2010). A statistic relating the economic condition to oral health showed that the chances of children from low income families suffering from cavities is almost twice (25%) than that of the children from higher income households (11%) (Dye, Li, & Beltrán-Aguilar, 2012).

Current Dental Imaging Techniques

X-ray is the current state of the art technique when it comes to dental imaging. They reveal information about the tooth structure as well as the surrounding bone and soft tissue. X-rays assist the clinician in providing information which maybe not be seen with just a visual examination. They can also aid as a diagnostic tool post treatment of the dental structure (Oliveira & Proença, 2011). X-ray dental imaging can be categorized into 2-D and 3-D X-ray. 2-D X-ray has been a

popular bio medical imaging tool since its discovery in 1895. 2-D X-ray can be divided into bitewing, periapical, and occlusal type of projections. However, 2-D X-ray imaging cannot access the area around the teeth. They also suffer from loss of spatial information due to 3-D object being constructed as a 2-D image. Another disadvantage of 2-D X-ray is that the object of interest, in this case the human teeth is obstructed due to the superimposition of its overlying structures (Shah, Bansal, & Logani, 2014). Additionally, one of the common dental defect, cracked tooth most often tends to be in the parallel direction of the radiographic plane, and hence is not captured in the radiographs (Mathew et al., 2012). Rarely occurring cracks on the buccolingual direction can be detected using radiographs. They also fail to provide correlation between the soft and the hard tissue. Recent advancements have given rise to more sophesticated 3-D X-ray devices such as the Cone Beam Computed Tomography (White, 2008). But the major concern of using 3-D X-ray is that the radiation exposure increases significantly. Also, it has very poor resolution when identifying thin dental cracks and craze lines. Moreover the total cost of a CT scan is much higher than the traditional radiographs (Shah et al., 2014).

Patients hesitate to use X-rays as the imaging modality due to the adverse effects of ionizing radiations in X-rays. Ionizing radiations are either particles or certain electromagnetic waves which have sufficient energy to remove electrons from an atom and thus ionizing the atom. These radiations are harmful to the human body and can ultimately lead to cancer (Radiation, 2000). A 2000 Report of the United Nations Scientific Committee on the Effects of Atomic Radiation to the General Assembly noted that in developed countries, the average level of exposure to ionizing radiation due to medical usage was approximately equal to 50% of the global average level of natural exposure (Radiation, 2000).

In dental imaging an alternative to the harmful ionizing X-rays, Magnetic Resonance Imaging (MRI) has been explored to detect and diagnose certain types of dental defects. An advantage that MRI has over X-ray is that it has better contrast sensitivity towards the soft tissues (Boeddinghaus & Whyte, 2008; Shah et al., 2014). However, MRI is known to be poor in distingushing between early benign stages of tumor and the later malignant tumor and may provide false-positive results (LaMarca et al., 2011; Shah et al., 2014). A major limitation of MRI is that patients with foriegn bodies containing ferromagnetic materials implanted in them, for example a pacemaker, cannot benefit from MRI as the ferromagnetic substance in the pacemaker would interact with the magnetic component of the MRI machine and could cause harm to the patient's body. In cases where patients suffere from claustrophobia, MRI machine may not be considered as an option. The scanning time for MRI is longer than that of X-ray imaging. In terms of cost, MRI is not cost effective (approx. $600-$2600) and costs more than the regular radiographic alternatives (Shah et al., 2014).

Like MRI, ultrasound imaging is a non-ionizing alternative to X-ray dental imaging (Marotti et al., 2013; Shah et al., 2014). Ultrasound technology was explored by Buam et al. in 1963 for dental imaging. A transducer with 15MHz was used, however the clarity of the radio frequency was not favorable. Studies have shown that it can be used for the early diagnosis of periodontal diseases. Ultrasound can be used to detect bony structures. However, in cases where structures beneath the bony surface has to be analyzed, ultrasound fails to identify the structure. Interpreting ultrasound images requires a highly trained and skilled ultrasound technician (Shah et al., 2014).

Fluorescence imaging is commonly used to visualize biological structures and processes. Due to difference in illumination as well as emission wavelength, fluorescence imaging technique

provides better contrast than traditional transillumination methods (Alander et al., 2012). Also, small quantity of the dye is required to make the structure under study visible thus providing better sensitivity (Alander et al., 2012). Indocyanine green (ICG) is an Food and Drug Administration (FDA) approved fluorescence dye, that has been used in the field of clinical as well as surgical imaging such as retinal angiography, study of the lymphatic system (Alander et al., 2012; Marshall et al., 2010) and cancer detection (Guyer et al., 1992; Kitai, Inomoto, Miwa, & Shikayama, 2005; Unno et al., 2008). Kodak Research Laboratories developed the ICG dye in 1955 for near-infrared imaging (Alander et al., 2012; Björnsson, Murphy, & Chadwick, 1982; Engel et al., 2008). Intravenous injected ICG was first used in early 1970 by Flower and Hochheimer to image choroidal circulation (Flower, 1972; Stanga, Lim, & Hamilton, 2003). In a study by Takeaki Ishizawa et al., ICG assisted microscopic examination was succesfully utilized to detect hepatocellular carcinoma (HCC) and colorectal carcinoma (CRC) (Ishizawa et al., 2009). Another study utilized near-infrared ICG fluorescence as a lymphographic technique in assessing lymph function (Unno et al., 2008). It is considered safe as it is low in toxicity value i.e. LD_{50} of 50–80 mg/kg for animals, where LD stands for lethal dose. Additionally, they are rapidly excreated into the bile (Alander et al., 2012; Hartzler, 2019). When illuminated with near-infrared light, ICG has a peak wavelength of 830nm. In human body, ICG binds to the plasma-protiens and these plasma protien then emit the peak wavelength light (Ishizawa et al., 2009; Landsman, Kwant, Mook, & Zijlstra, 1976). ICG assisted near-infrared fluorescence imaging has tissue penetration property. An added advantage is that it helps in real time visualization of the affected subject (Unno et al., 2008).

Near-Infrared Based Dental Imaging with ICG as Fluorescence Agent

To overcome the current limitations observed in X-ray, MRI and ultrasound dental imaging, this study concentrated on designing a novel experimental setup that exploits the advantages of ICG assisted near-infrared fluorecence imaigng. This design is a non-invasive, non-ionizing method that can be used to detect common dental diseses such as dental caries, dental decay as well as dental cracks. Near-infrared window I (650nm-950nm) as well as near-infrared window II (950nm-1700nm) were utilized in this study. Near-infrared is known to have reduced autoflourescence properties (Frangioni, 2003). Studies have shown that tissues have reduced absorption of the near-infrared light and good penetration (Maier, Walker, Fantini, Franceschini, & Gratton, 1994). Figure 2 helps in visualizing the electromagnetic spectrum and shows the wavelength range of near-infrared rays. It can also be observed (Figure 2) that the near-infrared wavelength falls under the longer wavelenght region in comparision to X-rays, which belong to the shorter wavelength region (1nm=0.001µm).

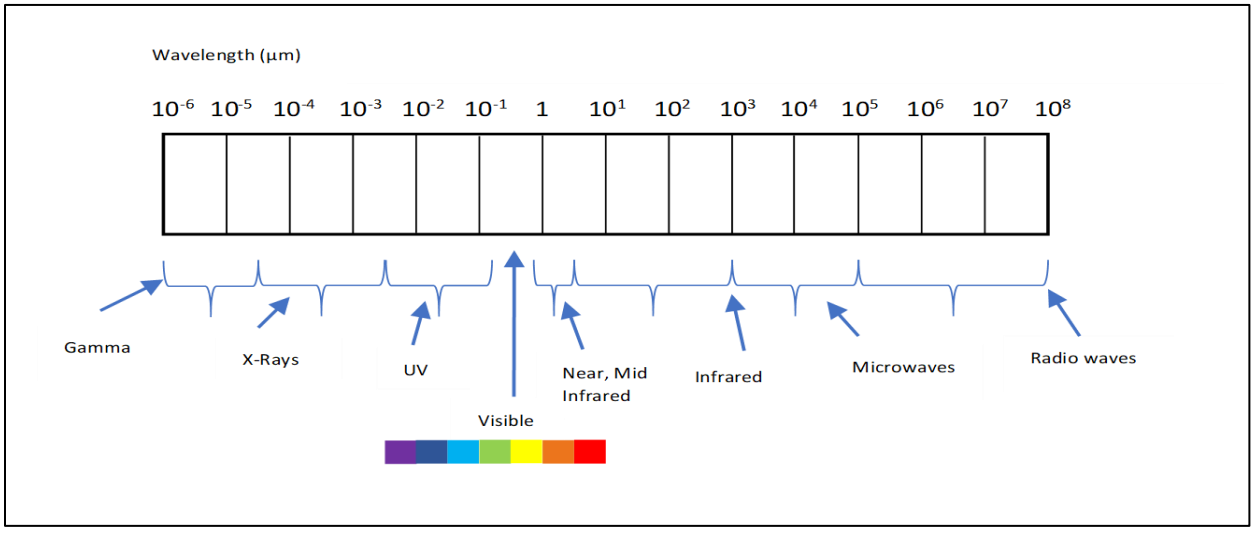

Figure 2. Schematic Diagram of the Electromagnetic Spectrum

A pilot dental imaging study was conducted on animal (rat) model (Li et al., 2018). It was a precurssor to this study. In the animal experimental model, an endoscopic imaging setup was

utilized to image unerrupted molars in the animal dental structure. The pilot study was successful in the detection of both erupted as well as unerupted molars since NIR light has tissue penetration properties. The study was taken further to optimize the imaging conditions for the rat (Hartzler, 2019; Li, Yao, & Xu, 2019). As animal molar structure have shown to have similarity to the human molar structure, the study by (Li et al., 2018) showed promising results for future human dental imaging.

The challenge in treatment of the dental diseases is their early detection and our method can be used for the early detection of dental cracks as well as caries (Li, Zaid, et al., 2019). Our previous study was the first to explore ICG assisted NIR dental imaging in the second NIR window (950nm-1700nm). It also helps in the early detection of cracked tooth, especially the craze lines. The total cost of our imaging set up is around $18,000 making it an affordable option in comparision to 3-D X-ray imaging equipment. This method also helps the clinician visualize the enamel-dentin boundary. Figure 3 provides an anatomical illustration of human tooth and can be utilized to visualize the enamel-dentin boundary. Also, the enamel becomes transparent when immersed in ICG and incident with the NIR light.

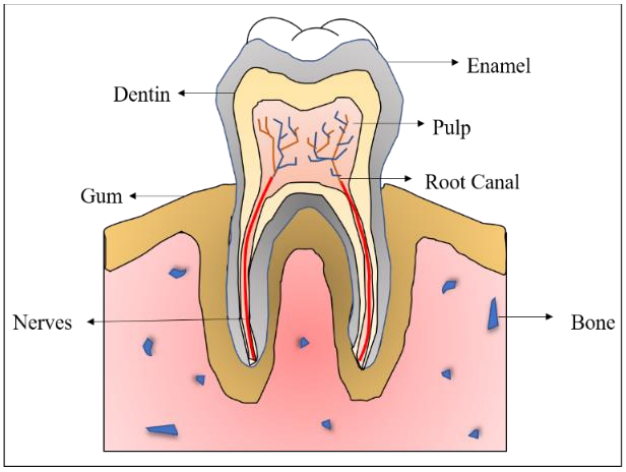

Figure 3. Anatomy of Human Dental Structure

MATERIAL AND IMAGING METHODOLOGY

Animal In-Vivo Imaging Setup

Animal (rat) study has been the precursor to this study (human) (Hartzler, 2019; Li, Yao, et al., 2019; Li et al., 2018). The imaging set up to capture the dental NIR fluorescence images consisted of the following key elements: near-infrared camera (NIR Camera), spectrometer, filters, endoscope and computer (Figure 4) (Li et al., 2018). The NIR light source used was a 785nm laser diode (Turnkey Raman Lasers-785 Series). A custom-made bifurcated endoscope (OSF-3; Olympus Corporation) was used to guide the laser light as well as capture the fluorescence from the dental structure. The spectrum of the fluorescence obtained is analyzed using a spectrometer (QEPro; Ocean Optics, Inc). A wide field camera (Guppy F038B; Allied Vision Technologies GmbH) with filters (band-pass: 800 nm) were used to capture the image and processed using a computer. The filters aided in removing the noise created due to background light and the near-infrared excitation. ICG powder, purchased from Sigma-Aldrich (St. Louis, USA), was diluted with ultrapure water (18.2 MΩ) at 1mg/mL concentration for the injection dose.

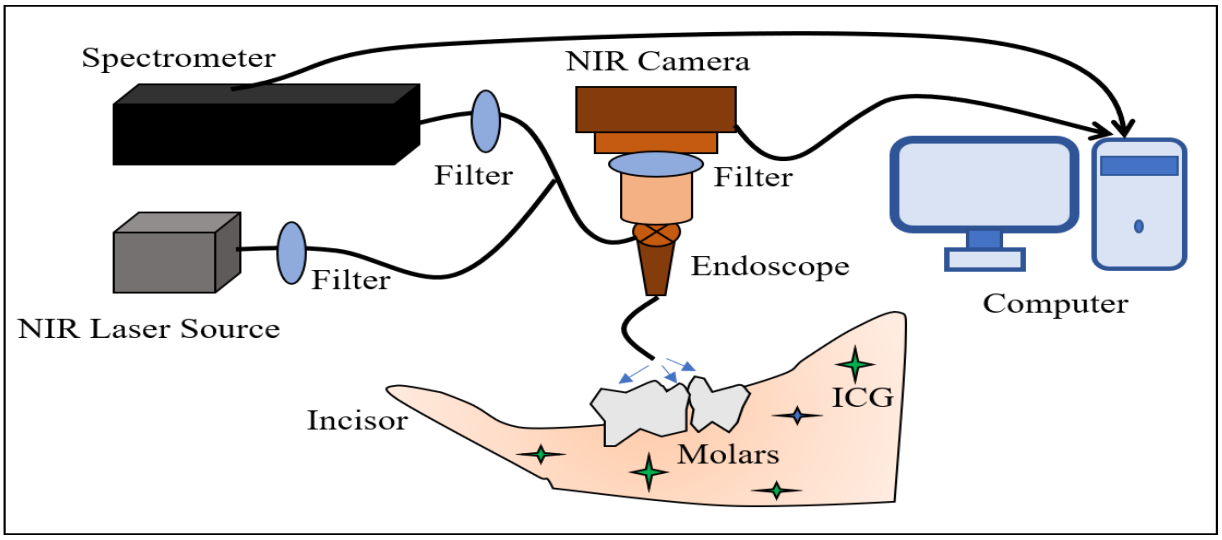

Figure 4. Animal ICG-NIRF Dental Imaging Setup

The rats used in the experimentation were Sprague-Dawley and were bred in the vivarium of the School of Veterinary Medicine, Louisiana State University. Due to their rapid as well as similar molar development model as humans, the rats were an ideal candidate for the pilot experimentation. All experiments were approved by the Institutional Animal Care and Use Committee of the Louisiana State University and in accordance to the ethical guidelines for animal care.

The imaging cycle were divided as per the eruption phase of the rat molars into unerupted molar phase and the erupted molar phase. The rat mandibles were extracted and were imaged using a wide field camera and an endoscope. The NIR images were then compared with 2-D X-ray as well as CT (SANCO Medical AG, model µCT 40).

Human Extracted Tooth Imaging Setup

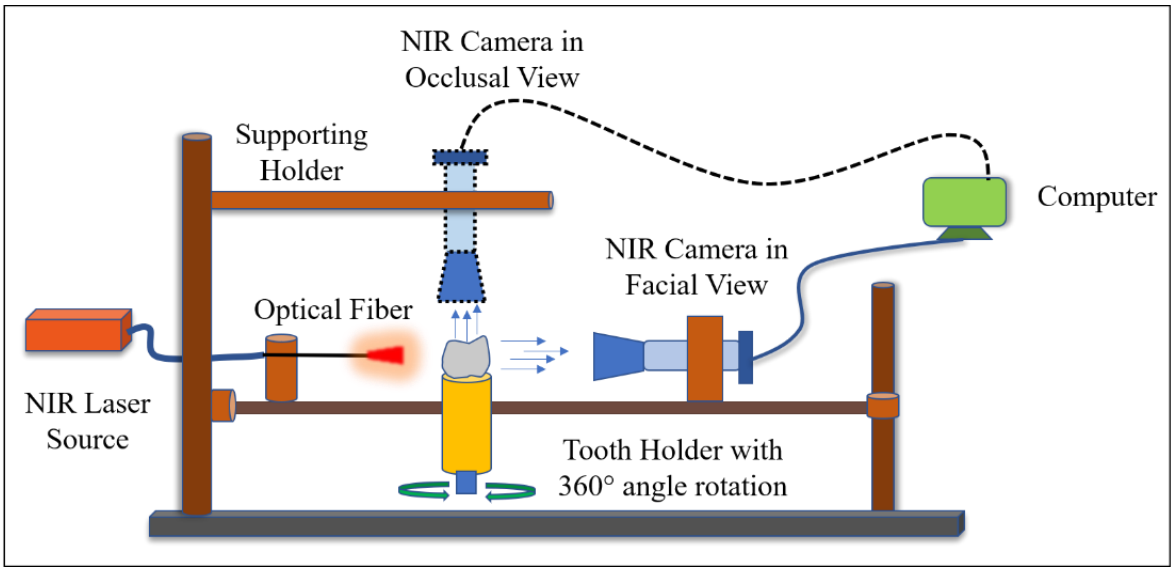

Figure 5. Extracted Human Tooth Experimental Setup

In this study we further explore the effects of ICG enhanced dental NIR imaging (ICG-NIRF) specific to detection of some common dental diseases such as dental cracks, dental caries as well as dental decays and comparing them with the images obtained from micro CT and 3-D

reconstructed X-ray images. The cracked teeth were collected from Louisiana State University Health Science Centre – Department of Oral and Maxillofacial Surgery (Baton Rouge, USA).

The reagents utilized were neutral buffer formalin solution, PBS (Phosphate Buffered Saline), ICG powder (Indocyanine Green) and ultra-pure water. Before imaging, the human teeth samples were subjected to 10% neutral buffer formalin solution and subsequently kept in PBS. Simultaneously, a 50 µM ICG solution was made with mixing ICG with ultra-pure water. The teeth were then stored in the 50 µM ICG solution for 24-hours. The next step was imaging the tooth.

The custom imaging platform seen in Figure 5 is similar to the previous animal experimental setup (Li et al., 2018). The key elements of the human experimental setup were as follows: Near-infrared laser, optical fiber, near-infrared camera (NIR Camera), tooth holder and a computer. The NIR light source consisted of a 785nm laser source as well as a 1300 nm laser source. The Y shaped optical fiber cable was used to focus the light to the exposed tooth. A tooth holder was utilized so the extracted dental structure could be rotated to 360°. The NIR camera with filters were utilized to capture the images. The computer was used to view and analyze the images. Imaging in NIR I (700nm-950nm) window requires a NIR laser diode with 785nm filter (bandpass lens: 785 nm, Thorlabs Inc) and the corresponding NIR camera used was Guppy F038B from Allied Vision Technologies GmbH, with an 800nm filter (long pass lens: 800 nm, Thorlabs Inc). The NIR II imaging source required a similar 785 nm laser, meanwhile the corresponding NIR II camera was an InGaAs camera (Goldeye G-008; Allied Vision Technologies GmbH) with 950 nm filter (long pass lens: 950nm; Thorlabs Inc). This study was in line with the ethical guidelines for human subjects of research and was approved by the Institutional Review Board of Louisiana State University (IRB#E11061).

The processing of the images was done in gray scale format as they were black and white images. The grayscale format is utilized quite often in image processing to analyze the intensity of light and it ranges from 0-255, 0 being black and 255 being white. In order to analyze contrast of the obtained NIR images an objective contrast parameter called intensity mean difference (IMD) was defined (Equation 1). It is the difference between the florescence intensity of the foreground and that of the background.

$$D_{mean\_diff} = avg(\sum_{i=0}^{n} \frac{(g_F - g_B)}{0.5*(\text{avg}(\sum_{i=0}^{n} g_F) + avg(\sum_{i=0}^{n} g_B))}) \quad (1)$$

Where g_F (foreground) and g_B (background) were the greyscale values of each individual pixel in the queues (line) of the foreground and background regions. n is the number of pixels in the measured queues (line) from the image.

A schematic describing the contrast calculation is show in Figure 6. For example, if the contrast of the cracked tooth must be observed, two parallel 2-dimensional lines were drawn across the obtained NIR images. One over the dental crack (CL) which is the foreground and the other slightly over to the side of the dental crack (BL) which is the background. The schematic of the tooth and the lines is observed in Figure 6 (a). Similarly, in order to calculate the contrast difference between the enamel and dentin, two parallel lines were drawn. One over the enamel region which is the foreground (FL) and the other on the dentin region which is the background (BL). The schematic of this can observed in Figure 6 (b).

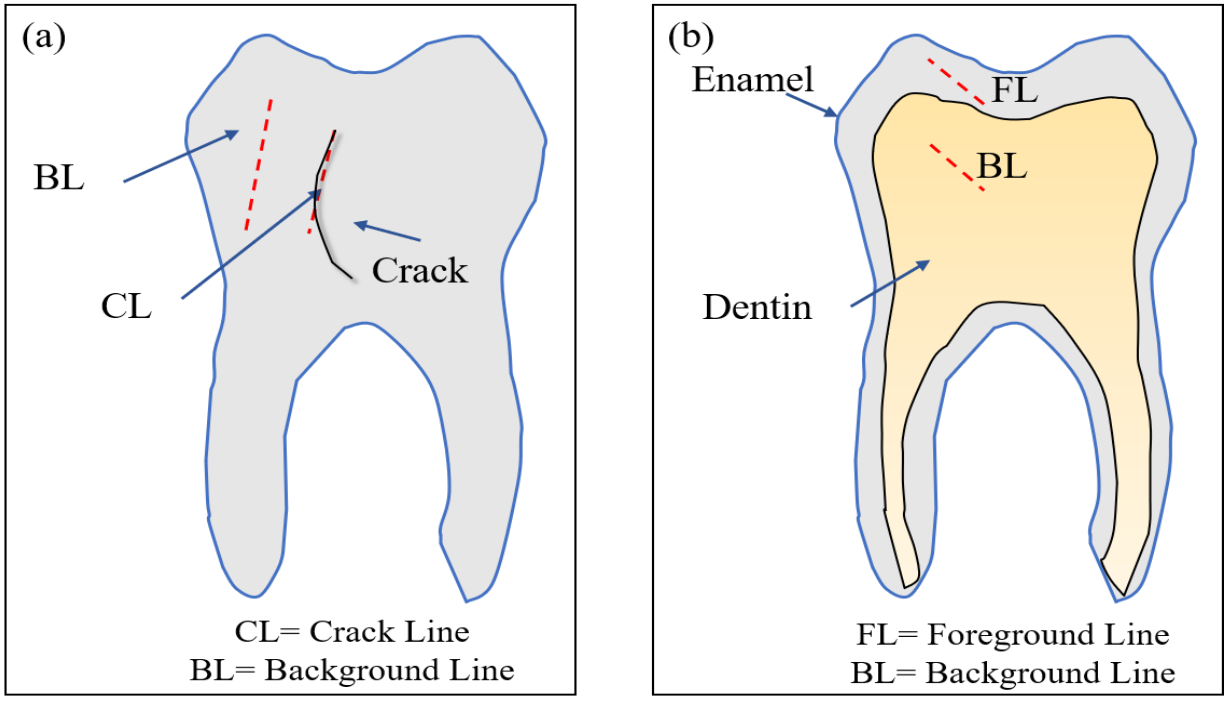

Figure 6. Schematic Diagram for the Contrast Calculation (a) Contrast Calculation Utilizing Background Line and Crack Line (b) Contrast Calculation Between Enamel and Dentin

X-Ray Imaging Equipment

For the comparative study with X-ray, the LSU School of Veterinary Medicine's micro CT machine (SCANCO Medical AG, model µCT 40) was utilized. The specifications for the micro CT device were 55 Kv, 144 µA and 300 ms of exposure. The resolution of the X-ray slices was 16 µm. Later, the 3-D reconstructed images were obtained using Avizo Software version 9.4.0 (Thermo Fisher Scientific).

Experimental Design

The experiment was designed to study the effect of ICG assisted near-infrared imaging in detecting common dental diseases and making a comparison with micro CT as well as the 3-D reconstructed X-ray. Some of the dental diseases analyzed were dental caries, dental decays as well as dental cracks. Another concept of study was analyzing the clear distinction between enamel-dentin junction as well as the effect of incident light angle on to the cracked tooth surface

in the better identification of the cracks. And lastly, an analysis of the time of immersion of the dental structure into the ICG solution as a factor contributing to the fluorescence light intensity as well as the image contrast was also studied.

RESULTS

Detection of Dental Cracks Through ICG-NIRF I and ICG-NIRF II Imaging Technique vs micro CT and 3-D Reconstructed X-ray

30 human dental structures were imaged using the ICG-NIRF technique (ICG assisted near-infrared imaging technique). The dental structures were also imaged through micro CT and the corresponding reconstructed 3-D images were obtained. The goal was to visualize the enamel cracks in the dental structure. The comparison between images obtained from 3-D X-ray and the ICG-NIRF technique revealed important results. Through the ICG-NIRF imaging technique the cracks on the enamel were clearly observed. Whereas, the same cracks in the enamel failed to be observed in the micro CT slices as well as the reconstructed 3D images. Figure 7 describes the comparison made between ICG-NIRF method and micro CT and their corresponding 3-D reconstructed X-ray. Figure 7 (a1) and (a2) show the dental structure under NIR window I and window II. The images obtained in both these windows were successful in identifying the enamel cracks. Their corresponding micro CT slice as well as the 3-D reconstructed images are seen in Figure 7 (a3), (a4). These images failed to observe the enamel cracks. Figure 7 (b1-b4) showcase another human dental structure imaged under the same conditions (i.e. ICG-NIRF vs X-ray) as the dental structure in Figure 7 (a1-a4). The results obtained showed that the ICG-NIRF method was successful in visualizing the enamel cracks whereas the corresponding micro CT and the 3-D reconstructed images failed in capturing the enamel cracks. The results presented in Figure 7 also conveyed that the study showed reproducible results on multiple tooth structure.

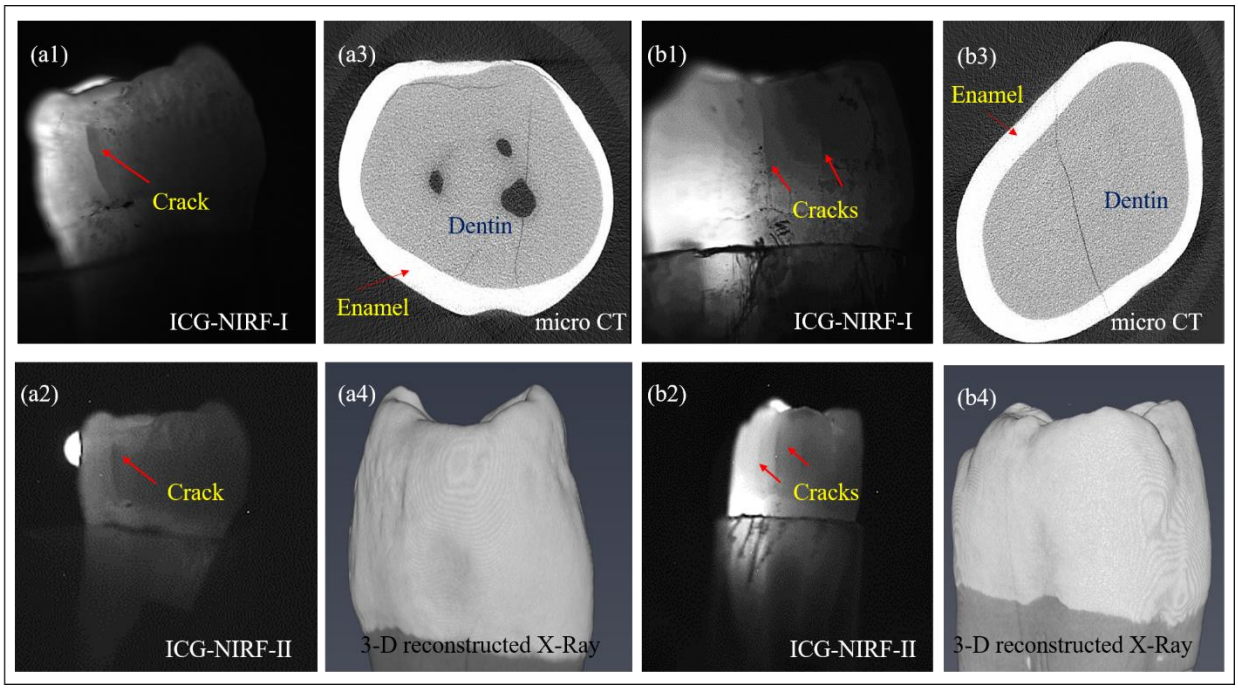

Figure 7. Visualization of the Enamel Cracks as Seen Through ICG-NIRF I and ICG-NIRF II in Comparison with micro CT and 3-D Reconstructed X-ray (a1) Dental Structure with Cracks Under ICG-NIRF I (a2) Dental Structure with Cracks Under ICG-NIRF II (a3) micro CT Slice (a4) Reconstructed 3-D Structure (b1-b4) Represent Similar Conditions as Seen Through Images (a1- a4) but for Another Human Dental Structure

Detection of Dental Caries and Decays Through ICG-NIRF I and ICG-NIRF II Imaging vs 3-D Reconstructed X-Ray Images

Dental structures affected with caries and decays were chosen as subjects for imaging with ICG-NIRF technique as well as 3-D reconstructed X-ray imaging technique. Figure 8 (a1) and (a2) show images of tooth structure with dental decay imaged using ICG-NIRF I and ICG-NIRF II respectively. Figure 8 (b1) (b2) show images of tooth structure with dental caries imaged using ICG-NIRF I and ICG-NIRF II respectively. The study was able to identify the dental caries as well as decays successfully. Dental decay is seen to have a predominant bright boundary in comparison to the rest of the tooth structure. Dental caries is seen as a bright dot in comparison to the background structure. This could be because of the ICG seeping into the caries. They (decay as well as caries) have been highlighted in Figure 8 using an orange rectangular box. Figure 8 (a3),

(b3) show the 3-D reconstructed X-ray images of the dental structure with decay and caries. The caries and decays can be observed as dark spots on the 3-D reconstructed images and have been highlighted using an orange rectangular box around it. This result shows that the ICG-NIRF dental imaging can produce comparable results to that of the 3-D reconstructed images without the harmful effects of X-ray.

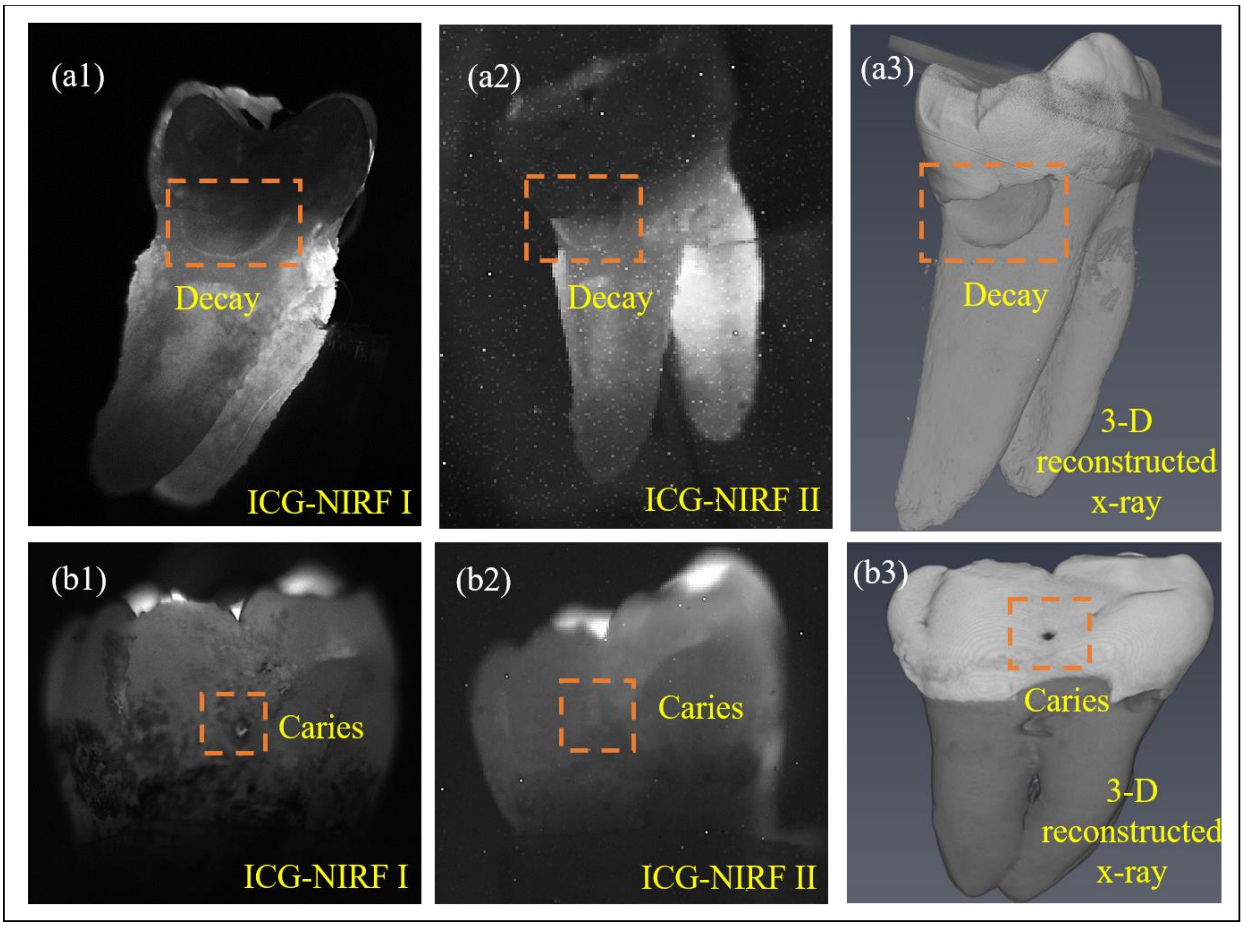

Figure 8. Visualization of Dental Decays and Dental Caries Through ICG-NIRF I and ICG-NIRF II and Comparing it with 3-D Reconstructed X-ray Images (a1-a2) Dental Decay as Seen Through ICG-NIRF I and ICG-NIRF II (a3) Dental Decay as Seen Through 3-D Reconstructed X-ray (b1-b2) Dental Caries as Seen Through ICG-NIRF I and ICG-NIRF II (b3) Dental Caries as Seen Through 3-D Reconstructed X-ray

Contrast vs ICG Immersion Time Window

Another major concept covered in this study is the effect of time of immersion on the contrast of the images. Immersion time for the extracted human dental structure can be defined as the amount of time the dental structure was immersed in the ICG solution before being imaged. The extracted human tooth was immersed in the ICG solution for a varied time interval ranging from as short as 1 minute to as long as 24 hours. The dental profiles at different immersion time and in the two NIR window i.e. window I and II were observed (Figure 9).

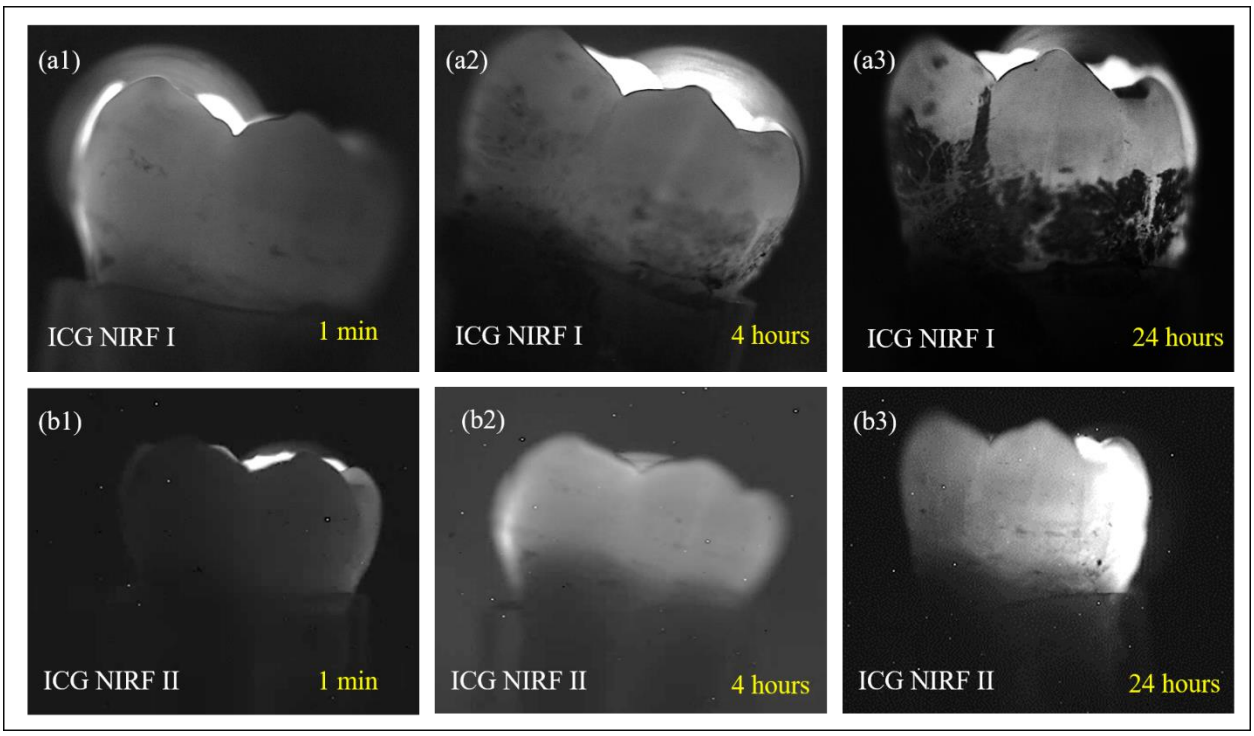

Figure 9. ICG Immersion and NIRF Imaging of the Dental Structures at Different Time Windows (a1) ICG-NIRF I at 1 minute (a2) ICG-NIRF I at 4 hours (a3) ICG-NIRF I at 24 hours (b1) ICG-NIRF II at 1 minute (b2) ICG-NIRF II at 4 hours (b3) ICG-NIRF II at 24 hours

Figure 9 (a1-a3) showed increasing time periods of immersion from 1 minute, 4 hours to 24 hours under ICG-NIRF window I. The same incremental immersion time is seen in Figure 9 (b1-b3) but under ICG-NIRF window II. As seen in Figure 9 (a1, b1) starting from 1 minute a satisfactory contrast was observed. As and when the immersion time increased, the contrast

increased as well and it can be observed in Figure 9 (a2, b2) for 4 hours of immersion and Figure 9 (a3, b3) for 24 hours of immersion. Figure 9 highlights the enamel clearly as a transparent structure. Figure 9 has been enhanced externally using Microsoft picture correction properties to make the dental structure clear to the human eye. Figure 10 shows a graph that describes the contrast vs time of immersion in ICG-NIRF I. The graph shows a substantial increase in the contrast with just a minute of immersion into the ICG solution. The contrast remains almost constant in the case of 1 minute, 4 hours as well as the 24-hour immersion. The contrast described was calculated using the concept of Intensity Mean Difference (IMD).

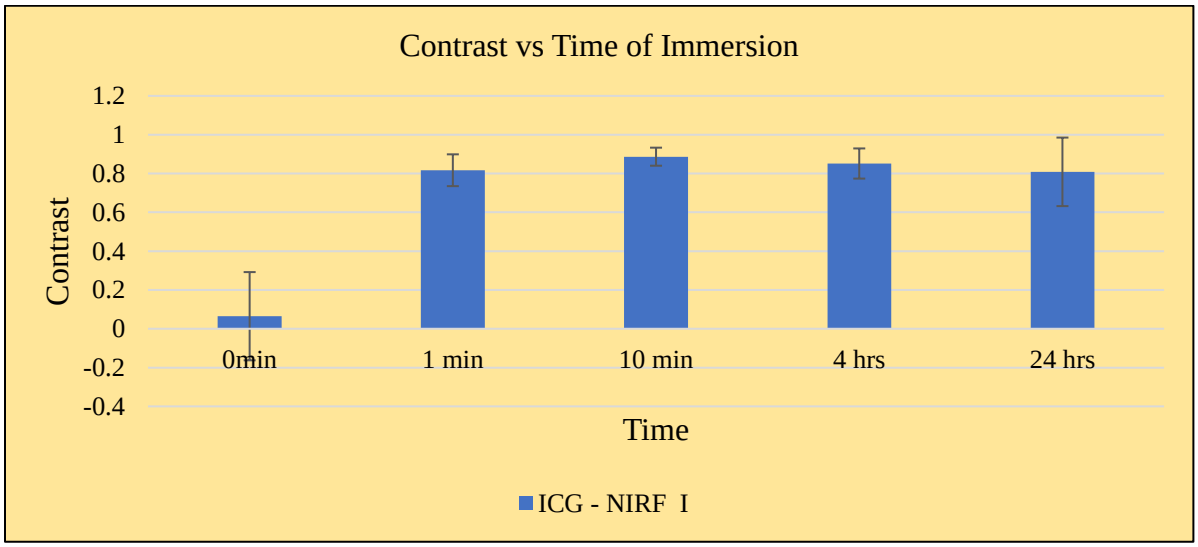

Figure 10. Image Contrast vs Time of Immersion of ICG(n=3), Where n is the Number of Teeth

Fluorescence Intensity vs ICG Immersion Time

Immersion time for the extracted human dental structure can be defined as the time period the dental structure is immersed in the ICG solution until its imaged. Different time period was chosen as the time of immersion starting from 0 minute, i.e. immediate immersion and imaging of the dental structure, to 24 hours i.e. an entire day of immersion before imaging of the dental structure. The time window of immersion influenced the ICG florescence intensity. The results show that intensity from the tooth with immediate ICG immersion and imaging was almost

negligible (Figure 11). However, when it was immersed in the ICG solution for a short duration, in this case a minute, the intensity increased exponentially (3663.79 a.u.). Subsequently, the intensity kept increasing and the maximum value (11286.69 a.u.) was obtained at 1 hour of immersion. The intensity then gradually begins to drop down and reaches 6021.01 a.u. at 24 hours of immersion.

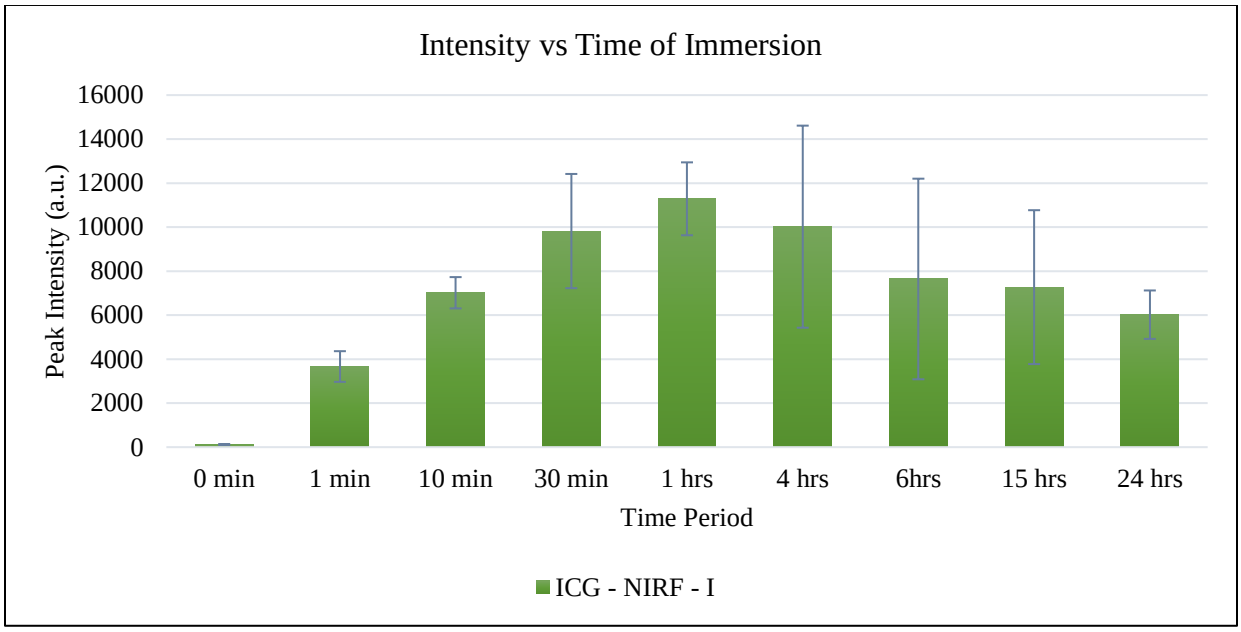

Figure 11. Fluorescence Intensity at Varied ICG Immersion Time(n=3), Where n is the Number of Teeth

Detection of Enamel-Dentin Junction Using ICG-NIRF I and ICG-NIRF II Window

The enamel-dentin junction was identified through ICG assisted NIRF imaging (Figure 12). The dental structure was immersed into the ICG for 1 minute, 4 hours and 24 hours respectively and imaged under NIR window I (650nm-950nm) (Figure 12 (a1-a3)). The same dental structure with the same immersion time were then imaged under the NIR window II (950nm-1700nm) (Figure 12 (b1-b3))

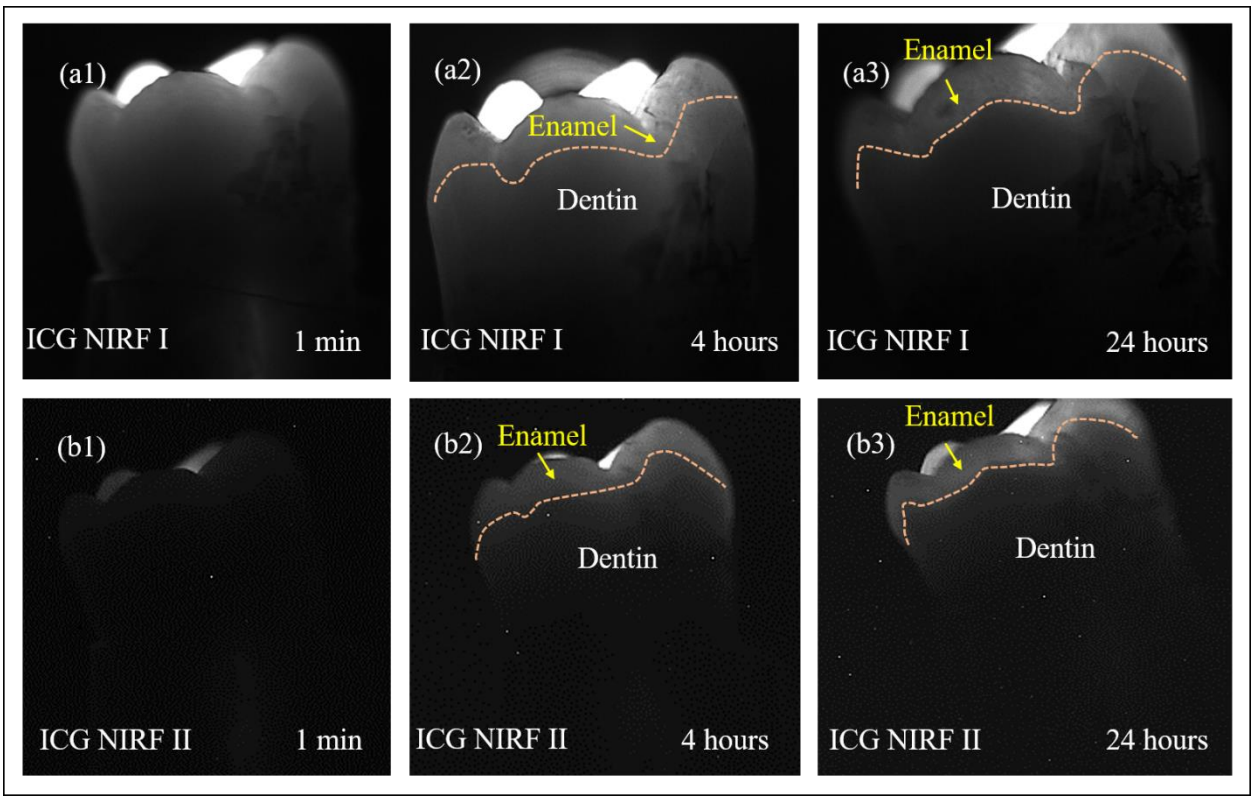

Figure 12. Detection of Enamel-Dentin Junction (a1) ICG-NIRF I at 1 minute (a2) ICG-NIRF I at 4 hours (a3) ICG-NIRF I at 24 hours (b1) ICG-NIRF II at 1 minute (b2) ICG-NIRF II at 4 hours (b3) ICG-NIRF II at 24 hours

It can be observed that both ICG-NIRF I as well as ICG-NIRF II were satisfactory in detecting the human tooth profile in a small imaging window, i.e. 1 minute. At the 4-hour immersion interval i.e. Figure 12 (a2) and (b2), the enamel-dentin boundary is clearly visible, and it improves as it moves on to 24-hour imaging window (Figure 12 (a3), (b3)). Also, human tooth profile in ICG-NIRF I is seen much clearly than in that of ICG-NIRF II. In Figure 12, the images have been enhanced externally using Microsoft picture correction properties to make the dental structures clear to the human eyes. A graph is plotted for both ICG-NIRF I as well as ICG-NIRF II between the immersion time i.e. 1 minute, 4 hours, 24 hours and their corresponding contrast (Figure 13). It is observed that for 24-hour immersion, the contrast is the highest. The contrast

was obtained by choosing the enamel as the foreground (FL) and the dentin as the background (BL) and a schematic diagram is seen in Figure 6.

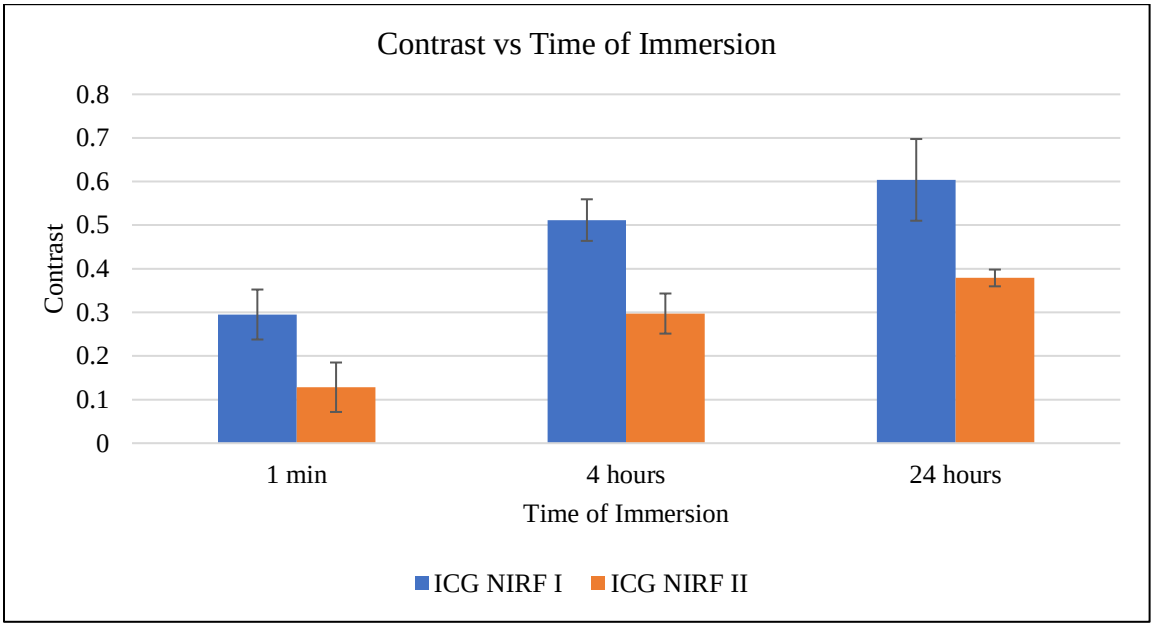

Figure 13. Imaging Contrast vs Different Time of Immersion for ICG-NIRF I and ICG-NIRF II

Effect of Angle of Light Exposure on the Contrast of the Image

The study concentrated on anlyzing the affect of the angle of light exposure on to the teeth for the detection of cracks. It was observed that the angled light exposure of a cracked tooth lead to an underlying shadow. This underlying shadow aided in the clear detection of the cracks. In the case where the light was angled in a parallel direction to that of the crack, there was no shadow formation and the corresponding crack detection was not clear. Figure 14 (a1), (b1) showed the schematic representation of an angled light exposure and parallel light exposure respectively. In the tooth with angled exposure i.e. in Figure 14 (a2), (a3), the images of the tooth in both ICG-NIRF-I as well as ICG-NIRF II showed good contrast as well as clear detection of the crack srtucture. However in the tooth with parallel exposure i.e. Figure 14 (b2), (b3) there was poor contrast as well as the cracks on the enamel were failed to be detected.

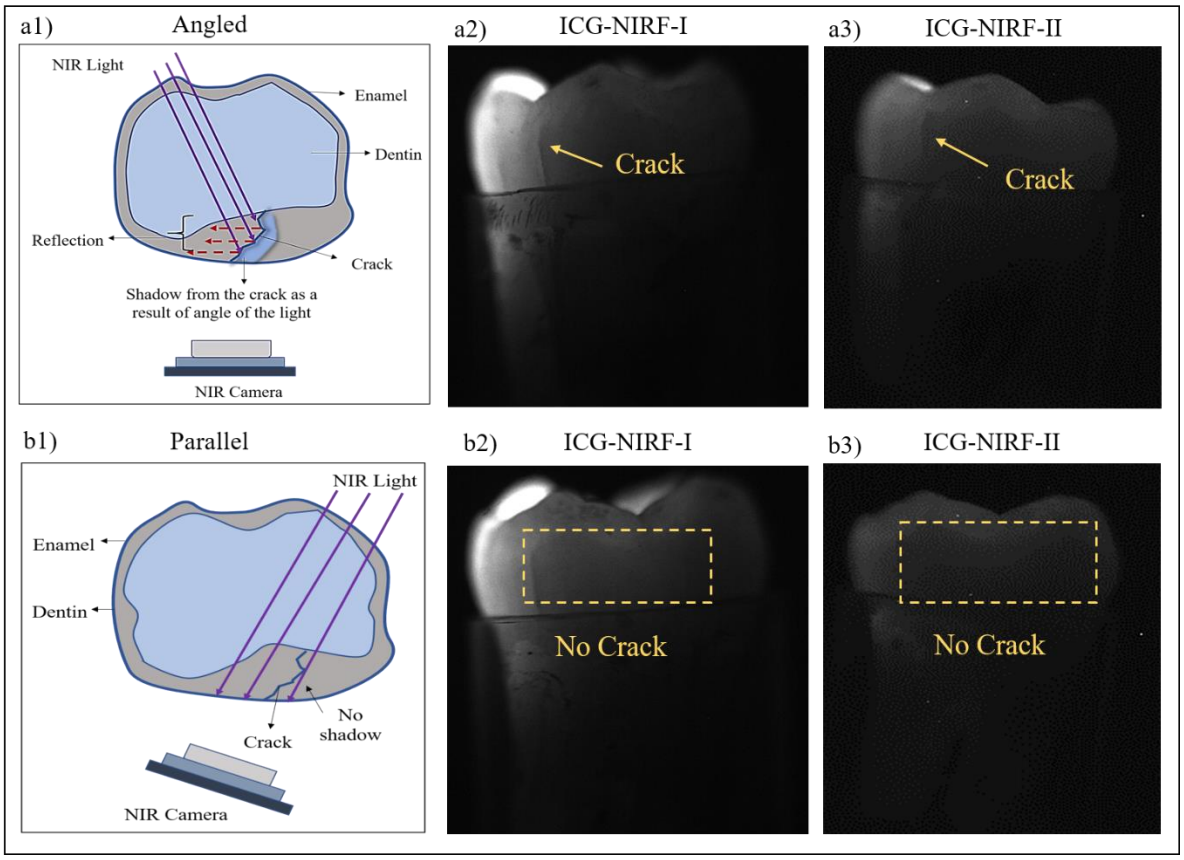

Figure 14. Angled vs Parallel Light Exposure (a1) Schematic Representation of the Angled Light Exposure and the Consequent Shadow Formation (a2) ICG-NIRF I Images of Dental Cracks Under Angled Light Exposure (a3) ICG-NIRF II Images of Dental Cracks Under Angled Light Exposure (b1) Schematic Representation of Parallel Angle of Light Exposure (b2) ICG-NIRF I Images of Dental Cracks Under Parallel Light Exposure (b3) ICG-NIRF II Images of Dental Cracks Under Parallel Light Exposure

Figure 15 provides a graphical representation of the contrast with respect to the angled light exposure and parallel light exposure. The contrast of the cracked tooth was observed by drawing two parallel 2-dimensional lines across the obtained NIR images. One over the dental crack (CL) which is the foreground and the other slightly over to the side of the dental crack (BL) which is the background (Figure 6).

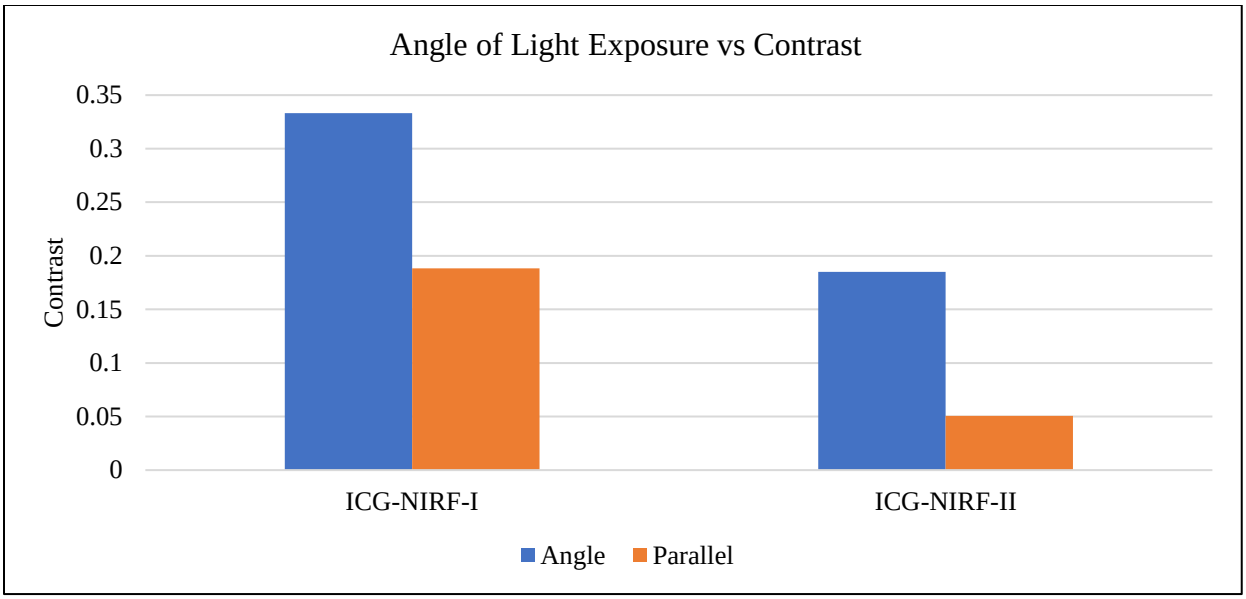

Figure 15. Contrast vs Angle of Light Exposure on Cracked Tooth in Both ICG-NIRF I and ICG-NIRF II Window

Through the graph it can be seen that the contrast through both ICG-NIRF I and ICG-NIRF II in an angled exposure is higher than that of the parallel exposure. This indicates that the angled direction of the light on to the tooth structure aides in a better contrast and also increases the chance of detecting cracks on the enamel.

DISCUSSION

Oral health is of utmost importance in ensuring the persons overall health (Benjamin, 2010; McGrath & Bedi, 2004). Early detection of dental diseases gives both the patient as well as the clinician an edge when it comes to creating a treatment plan and stopping the progress of the disease. Dental imaging is a useful tool that aids in the detection and diagnosis of dental diseases in their preliminary stages. The current state of the art dental imaging technology i.e. X-ray fails in the detection of some of the common dental diseases due to a variety of reasons, some of them being loss of spatial information and artifacts such as geometrical distortion when conversion from 2-D to 3-D images (Correa et al., 2014; Rondon, Pereira, & do Nascimento, 2014; Shah et al., 2014). Dental fractures fail to be detected in 3-D X-rays (Computed Tomography-CT) as the resolution of the CT is lower than that of the fractures (Shah et al., 2014). They also highly rely on the position of the patient to detect the dental disease (Rondon et al., 2014). This study utilized ICG assisted near-infrared dental imaging to visualize the dental diseases such as cracks, caries as well as decays. The results observed through Figure 7 shows the clear identification of dental cracks through ICG-NIRF I and ICG-NIRF II, however the 3-D reconstructed images failed to show the same cracks. This in turn implies that the experimental setup has a potential of being used as the diagnostic tool when a cracked tooth is suspected in a patient. The study also showed successful results in the detection of dental decays as well as dental caries (Figure 8). Increased immersion time showed increased contrast as well as increased fluorescence intensity (Figure 10, Figure 11). The enamel-dentin junction was seen clearly as the enamel turned transparent (Figure 12) as well as good contrast was seen between the enamel and dentin (Figure 13). It is know that craze lines usually begin in the enamel region (Mariona & Antony, 2018). This implies that if ICG-NIRF technique is utilized by a clinician suspecting craze lines, they can locate them due to clear

enamel-dentin differentiation. Also, this study analyzed the effect of an angled exposure of light onto the cracks (Figure 14). It was observed that with an angled exposure of light onto the crack a shadow is formed. This shadow helped in improving the contrast of the crack detection (Figure 15). These results emphasize that this study was successful in overcoming the limitation of X-ray in the detection of common dental diseases.

One of the major concerns of patients on using X-ray to diagnose dental diseases is the harmful effects of X-rays on to the human body (Angelino, Edlund, & Shah, 2017). In cases of pregnant women, X-ray poses special challenges. Although studies show that doses within limit i.e. less than 5 rads does not affect the fetus (Ratnapalan, Bona, Koren, & Team, 2003; Wrzosek & Einarson, 2009), practitioners are often hesitant in using X-ray dental images on pregnant women. Studies also show that in cases of emergencies approximately 36-46% of the clinicians refuse to take X-rays on pregnant women (Abbott, 2000; Monsour, Kruger, Barnes, & Sainsbury, 1988). This puts pregnant women on a diagnostic disadvantage when it comes to detecting dental diseases. In cases where panoramic X-ray is required, patient positioning is a major factor that could contribute to errors in the dental imaging (Rondon et al., 2014). Incorrect positioning can result in misdiagnosis of the disease and can lead to multiple images being taken that can increase the exposure risk to the patient (Rondon et al., 2014). This study was able to identify dental cracks (Figure 7), dental decays as well as dental caries (Figure 8) successfully by utilizing non-ionizing radiation (near-infrared). The results of dental decays and caries detection (Figure 8) showcase that the results are comparable to that obtained from 3-D reconstructed X-ray images. Also, ICG-NIRF technique offers the advantage of real-time dental imaging, i.e. the clinician can visualize the dental structure without any wait time.

Traditional bitewing X-ray films have a size anywhere between 2-7 cm (Pandula) and the patient needs to bite it in order to hold the film in position. This could lead to patient discomfort. In cases where children require bitewing it may be difficult for them to hold the film in place. As mentioned previously, the position of the patient is crucial when it comes to X-ray dental imaging. X-ray also requires the patient to be still during the imaging session in order to avoid errors. However, when children are required to take dental X-rays, they may find it difficult to stay in the perfect position conducive for X-ray imaging. This study does not require an intra oral film placement. Additionally, the source of light is the only device placed internal to the oral cavity which can be very easily maneuvered by the clinician using an endoscope. The tip of the endoscope utilized in this study is approximately 2 mm. In comparison to the bitewing film, the tip of the endoscope is approximately 10 times smaller. Hence, the patient need not be extremely still, thus reducing the level of discomfort to a great extent. In comparison to MRI technique, the patient need not be enclosed in a closed space in ICG-NIRF imaging. Hence the population with claustrophobia can be imaged using this technique. Since MRI interacts with ferromagnets, people with ferromagnetic implants cannot be subjected to MRI. However, ICG-NIRF has no reaction with ferromagnetic substances and hence can be used to image patients with ferromagnetic implants.

The cost of ICG-NIRF imaging set up is around $18,000. The camera system (including NIR I and NIR II cameras) approximately costs $10,000 and the laser source costs approx. $8000. The 2-D X-ray equipment costs around $50,000-$95,000 and 3-D X-ray costs around $160,000-$300,000 (LoVette, 2019). This makes our equipment cost 5-16 times lesser than X-ray equipment. The session cost of X-ray imaging can be anywhere between $10-$250 (Unkown, 2019a). In ICG-NIRF imaging, the cost of ICG is an important factor in terms of analyzing the session cost.

Pharmaceutical grade ICG costs approximately $76 for 25mg (Unkown, 2019b). When compared with X-ray session cost, the cost of purchasing ICG is considerably lower. A 1.5-3T MRI equipment costs anywhere between $1-$3 million and an individual scan can cost anywhere between $600-$2600 (Reed, 2019). In comparison, ICG-NIRF equipment as well as the session cost is much lower. Hence, ICG-NIRF dental imaging technique can be considered as a cost-effective option in comparison to 2-D X-rays, 3-D X-rays as well as MRI.

CONCLUSION

To summarize, this study concentrated on detecting some of the common dental diseases utilizing ICG-NIRF imaging technique and making a comparison with the state-of-the-art micro CT as well as 3-D reconstructed X-ray imaging techniques. Dental cracks were observed successfully utilizing the ICG-NIRF method whereas the 3-D reconstructed X-ray images failed to detect the cracks. Micro CT detected the dentin cracks but as the crack progressed into the enamel it failed in detecting them. The clear detection of enamel is an advantage of using near-infrared light. The increased time of immersion of ICG improved the contrast of the enamel. The enamel-dentin junction was also clearly visualized due to ICG immersion of the dental structure and imaged through NIRF imaging. This improved enamel contrast can assist in the detection of craze lines, which is the beginning stage of a cracked tooth and are usually present in enamel. Additionally, the study was successful in identifying dental diseases such as dental caries as well as dental decays. The effect on fluorescence intensity as well as contrast with varying immersion time was examined in this study. It was found that as the time of immersion increased, the fluorescence intensity as well as the contrast increased. This study also laid emphasis on the importance of the angle of exposure to detect the cracks. In the case of dental cracks, the clinician not only needs to know the existence of a crack, but also their location and depth. In the future, the depth analysis of the cracks can be conducted using the angled NIR light exposure to obtain a shadow from the cracks (Zhongqiang Li). The imaging set up is cost affective in comparison to 3-D X-ray machines. The compact size of the imaging set up can aid the clinician and provide a comfortable setting for the patient as well. In conclusion, the study has proven to be a successful non-ionizing, non-invasive dental imaging method that could be used by the clinicians in the future.

Currently, there are certain disadvantages to the ICG assisted near-infrared technique. Although it provided good enamel detection, it is not successful in detecting diseases and defects in the dentin. This means that if a dental disease originates internally, i.e. in the pulp or dentin, the ICG assisted technique would not be able to diagnose it. Also, in the case of cracked tooth further study is required to calculate the depth of the detected cracks (Zhongqiang Li) . In the future, for the human dental structure imaging, an ICG mouth wash may be utilized (Zheng Li Unpublished). ICG-NIRF method is not label free and the patients may be apprehensive to come in contact with ICG. It is suspected that in case of in-vivo experimentation, the saliva in the human oral cavity could interfere with the current experimental criteria. This study in the future will be expanded to study the detection of other common dental diseases such as periodontal diseases as well as abscess. This study has scope to be further improved in order to account for the current draw backs.

APPENDIX. IRB FORM

ACTION ON EXEMPTION APPROVAL REQUEST

Institutional Review Board
Dr. Dennis Landin, Chair
130 David Boyd Hall
Baton Rouge, LA 70803
P: 225.578.8692
F: 225.578.5983
irb@lsu.edu
lsu.edu/research

TO: Jian Xu
Electrical and Computer Engineering

FROM: Dennis Landin
Chair, Institutional Review Board

DATE: April 26, 2018

RE: IRB# E11061

TITLE: Imaging extracted teeth with indocyanine green

New Protocol/Modification/Continuation: New Protocol

Review Date: 4/26/2018

Approved X **Disapproved**_____

Approval Date: 4/26/2018 **Approval Expiration Date:** 4/25/2021

Exemption Category/Paragraph: 4a

Signed Consent Waived?: N/A

Re-review frequency: (three years unless otherwise stated)

LSU Proposal Number (if applicable):

Protocol Matches Scope of Work in Grant proposal: (if applicable)

By: Dennis Landin, Chairman

PRINCIPAL INVESTIGATOR: PLEASE READ THE FOLLOWING –
Continuing approval is CONDITIONAL on:

1. Adherence to the approved protocol, familiarity with, and adherence to the ethical standards of the Belmont Report, and LSU's Assurance of Compliance with DHHS regulations for the protection of human subjects*
2. Prior approval of a change in protocol, including revision of the consent documents or an increase in the number of subjects over that approved.
3. Obtaining renewed approval (or submittal of a termination report), prior to the approval expiration date, upon request by the IRB office (irrespective of when the project actually begins); notification of project termination.
4. Retention of documentation of informed consent and study records for at least 3 years after the study ends.
5. Continuing attention to the physical and psychological well-being and informed consent of the individual participants, including notification of new information that might affect consent.
6. A prompt report to the IRB of any adverse event affecting a participant potentially arising from the study.
7. Notification of the IRB of a serious compliance failure.
8. **SPECIAL NOTE: When emailing more than one recipient, make sure you use bcc. Approvals will automatically be closed by the IRB on the expiration date unless the PI requests a continuation.**

* *All investigators and support staff have access to copies of the Belmont Report, LSU's Assurance with DHHS, DHHS (45 CFR 46) and FDA regulations governing use of human subjects, and other relevant documents in print in this office or on our World Wide Web site at http://www.lsu.edu/irb*

REFERENCES

Abbott, P. (2000). Are dental; radiographs safe? *Australian Dental Journal, 45*(3), 208-213.

Alander, J. T., Kaartinen, I., Laakso, A., Pätilä, T., Spillmann, T., Tuchin, V. V., . . . Välisuo, P. (2012). A review of indocyanine green fluorescent imaging in surgery. *Journal of Biomedical Imaging, 2012*, 7.

Angelino, K., Edlund, D. A., & Shah, P. (2017). Near-Infrared Imaging for Detecting Caries and Structural Deformities in Teeth. *IEEE journal of translational engineering in health and medicine, 5*, 2300107-2300107. doi:10.1109/JTEHM.2017.2695194

Banerji, S., Mehta, S., & Millar, B. (2010). Cracked tooth syndrome. Part 1: aetiology and diagnosis. *British dental journal, 208*(10), 459.

Benjamin, R. M. (2010). Oral health: the silent epidemic. *Public health reports, 125*(2), 158.

Björnsson, Ó. G., Murphy, R., & Chadwick, V. (1982). Physicochemical studies of indocyanine green (ICG): absorbance/concentration relationship, pH tolerance and assay precision in various solvents. *Experientia, 38*(12), 1441-1442.

Blas, E., & Kurup, A. S. (2010). *Equity, social determinants and public health programmes*: World Health Organization.

Boeddinghaus, R., & Whyte, A. (2008). Current concepts in maxillofacial imaging. *European journal of radiology, 66*(3), 396-418.

Cadman, B. (2018, June 1 2018). Cracked tooth: Symptoms, diagnosis, and treatment. Retrieved from https://www.medicalnewstoday.com/articles/322015.php

Cadman, B. (2018). How do you know if you have a cracked tooth?

Coleman, P. (2002). Improving oral health care for the frail elderly: a review of widespread problems and best practices. *Geriatric Nursing, 23*(4), 189-198.

Correa, L. R., Spin-Neto, R., Stavropoulos, A., Schropp, L., da Silveira, H. E. D., & Wenzel, A. (2014). Planning of dental implant size with digital panoramic radiographs, CBCT-generated panoramic images, and CBCT cross-sectional images. *Clinical oral implants research, 25*(6), 690-695.

Da Rosa, W. L. d. O., Pradebon, L., Brondani, T. M. D. S., Piva, E., & Da Silva, A. F. (2017). Diagnosis and Treatment of Anterior Cracked Tooth: A Case Report.

Dye, B. A., Li, X., & Beltrán-Aguilar, E. D. (2012). Selected oral health indicators in the United States, 2005-2008.

Engel, E., Schraml, R. d., Maisch, T., Kobuch, K., König, B., Szeimies, R.-M., . . . Vasold, R. (2008). Light-induced decomposition of indocyanine green. *Investigative ophthalmology & visual science, 49*(5), 1777-1783.

Fleming, E., & Afful, J. (2018). Prevalence of total and untreated dental caries among youth: United States, 2015–2016.

Flower, R. W. (1972). Infrared absorption angiography of the choroid and some observations on the effects of high intraocular pressures. *American journal of ophthalmology, 74*(4), 600-614.

Frangioni, J. V. (2003). In vivo near-infrared fluorescence imaging. *Current opinion in chemical biology, 7*(5), 626-634.

Guyer, D. R., Puliafito, C. A., Monés, J. M., Friedman, E., Chang, W., & Verdooner, S. R. (1992). Digital Indocyanine-green Angilography in Chorioretinal Disorders. *Ophthalmology, 99*(2), 287-291.

Hartzler, T. (2019). Design and Optimization of an Ionizing-Radiation-Free Dental Imaging Scheme by Near Infrared Fluorescence.

Hasan, S., Singh, K., & Salati, N. (2015). Cracked tooth syndrome: overview of literature. *International Journal of Applied and Basic Medical Research, 5*(3), 164.

Ishizawa, T., Fukushima, N., Shibahara, J., Masuda, K., Tamura, S., Aoki, T., . . . Kokudo, N. (2009). Real-time identification of liver cancers by using indocyanine green fluorescent imaging. *Cancer, 115*(11), 2491-2504.

Kitai, T., Inomoto, T., Miwa, M., & Shikayama, T. (2005). Fluorescence navigation with indocyanine green for detecting sentinel lymph nodes in breast cancer. *Breast cancer, 12*(3), 211-215.

LaMarca, B., Speed, J., Ray, L. F., Cockrell, K., Wallukat, G., Dechend, R., & Granger, J. (2011). Hypertension in response to IL-6 during pregnancy: role of AT1-receptor activation. *International journal of interferon, cytokine and mediator research: IJIM, 2011*(3), 65.

Landsman, M., Kwant, G., Mook, G., & Zijlstra, W. (1976). Light-absorbing properties, stability, and spectral stabilization of indocyanine green. *Journal of applied physiology, 40*(4), 575-583.

Li, Z., Yao, S., & Xu, J. (2019). Indocyanine-green-assisted near-infrared dental imaging-the feasibility of in vivo imaging and the optimization of imaging conditions. *Scientific reports, 9*(1), 8238.

Li, Z., Yao, S., Xu, J., Wu, Y., Li, C., & He, Z. (2018). Endoscopic near-infrared dental imaging with indocyanine green: a pilot study. *Annals of the New York Academy of Sciences, 1421*(1), 88-96.

Li, Z., Zaid, W., Hartzler, T., Ramos, A., Osborn, M. L., Li, Y., . . . Xu, J. (2019). Indocyanine green–assisted dental imaging in the first and second near-infrared windows as compared with X-ray imaging. *Annals of the New York Academy of Sciences*.

LoVette, D. (2019). 3 Price Points For Digital X-Ray Equipment Options. Retrieved from https://info.blockimaging.com/bid/72486/3-price-points-for-digital-x-ray-equipment-options.

Lubisich, E. B., Hilton, T. J., Ferracane, J., & Northwest, P. (2010). Cracked teeth: a review of the literature. *Journal of esthetic and restorative dentistry : official publication of the American Academy of Esthetic Dentistry ... [et al.], 22*(3), 158-167. doi:10.1111/j.1708-8240.2010.00330.x

Maier, J. S., Walker, S. A., Fantini, S., Franceschini, M. A., & Gratton, E. (1994). Possible correlation between blood glucose concentration and the reduced scattering coefficient of tissues in the near infrared. *Optics letters, 19*(24), 2062-2064.

Mariona, R. P., & Antony, S. D. P. (2018). Diagnostic methods for cracked tooth by two endodontic tools. *dentist, 8*, 15.

Marotti, J., Heger, S., Tinschert, J., Tortamano, P., Chuembou, F., Radermacher, K., & Wolfart, S. (2013). Recent advances of ultrasound imaging in dentistry–a review of the literature. *Oral surgery, oral medicine, oral pathology and oral radiology, 115*(6), 819-832.

Marshall, M. V., Rasmussen, J. C., Tan, I.-C., Aldrich, M. B., Adams, K. E., Wang, X., . . . Sevick-Muraca, E. M. (2010). Near-infrared fluorescence imaging in humans with indocyanine green: a review and update. *Open surgical oncology journal (Online), 2*(2), 12.

Mathew, S., Thangavel, B., Mathew, C. A., Kailasam, S., Kumaravadivel, K., & Das, A. (2012). Diagnosis of cracked tooth syndrome. *Journal of pharmacy & bioallied sciences, 4*(Suppl 2), S242-S244. doi:10.4103/0975-7406.100219

McGrath, C., & Bedi, R. (2004). A national study of the importance of oral health to life quality to inform scales of oral health related quality of life. *Quality of Life Research, 13*(4), 813-818.

Merskey, N. (1994). Classificaiton of chronic pain; Description of chronic pain syndromes and definitions of pain Terms. *Task force on taxonomy of the International Association for the study of pain*, 41-43.

Monsour, P., Kruger, B., Barnes, A., & Sainsbury, A. (1988). Measures taken to reduce X-ray exposure of the patient, operator, and staff. *Australian Dental Journal, 33*(3), 181-192.

Oliveira, J., & Proença, H. (2011). Caries detection in panoramic dental X-ray images *Computational Vision and Medical Image Processing* (pp. 175-190): Springer.

Pandula, V. Different Types and Sizes of X-ray Films-Dentistry. Retrieved from https://www.juniordentist.com/types-and-sizes-of-xray-films.html

Petersen, P. E. (2003). The World Oral Health Report 2003: continuous improvement of oral health in the 21st century–the approach of the WHO Global Oral Health Programme. *Community Dentistry and oral epidemiology, 31*, 3-24.

Petersen, P. E. (2004). Improvement of oral health in Africa in the 21st century-the role of the WHO Global Oral Health Programme. *African Journal of Oral Health, 1*(1), 2-16.

Radiation, U. N. S. C. o. t. E. o. A. (2000). *Sources and effects of ionizing radiation: sources* (Vol. 1): United Nations Publications.

Ratnapalan, S., Bona, N., Koren, G., & Team, M. (2003). Ionizing radiation during pregnancy. *Canadian Family Physician, 49*(7), 873-874.

Reed, E. (2019). How Much Does An MRI Cost? *Thestreet.* Retrieved from https://www.thestreet.com/lifestyle/health/how-much-does-an-mri-cost-14972340.

Rivera, E., & Walton, R. (2008). Cracking the cracked tooth code: detection and treatment of various longitudinal tooth fractures. *Am Assoc Endodontists Colleagues for Excellence News Lett, 2*, 1-19.

Rondon, R. H. N., Pereira, Y. C. L., & do Nascimento, G. C. (2014). Common positioning errors in panoramic radiography: A review. *Imaging science in dentistry, 44*(1), 1-6.

Shah, N., Bansal, N., & Logani, A. (2014). Recent advances in imaging technologies in dentistry. *World journal of radiology, 6*(10), 794.

Stanga, P. E., Lim, J. I., & Hamilton, P. (2003). Indocyanine green angiography in chorioretinal diseases: indications and interpretation: an evidence-based update. *Ophthalmology, 110*(1), 15-21.

TÜRp, J. C., & Gobetti, J. P. (1996). THE CRACKED TOOTH SYNDROME: AN ELUSIVE DIAGNOSIS. *The Journal of the American Dental Association, 127*(10), 1502-1507. doi:10.14219/jada.archive.1996.0060

Unkown. (2019a). How Much Do Dental X-Rays Cost? - Costhelper.Com. Retrieved from https://health.costhelper.com/dental-x-ray.html.

Unkown. (2019b). Indocyanine Green Prices, Coupons & Patient Assistance Programs - Drugs.Com. Retrieved from https://www.drugs.com/price-guide/indocyanine-green.

Unno, N. a., Nishiyama, M., Suzuki, M., Yamamoto, N., Inuzuka, K., Sagara, D., . . . Konno, H. (2008). Quantitative lymph imaging for assessment of lymph function using indocyanine green fluorescence lymphography. *European Journal of Vascular and Endovascular Surgery*, *36*(2), 230-236.

Vos, T., Abajobir, A. A., Abate, K. H., Abbafati, C., Abbas, K. M., Abd-Allah, F., . . . Abera, S. F. (2017). Global, regional, and national incidence, prevalence, and years lived with disability for 328 diseases and injuries for 195 countries, 1990–2016: a systematic analysis for the Global Burden of Disease Study 2016. *The Lancet*, *390*(10100), 1211-1259.

White, S. C. (2008). Cone-beam imaging in dentistry. *Health physics*, *95*(5), 628-637.

WorldHealthOrganization. (2018). Oral health.

Wrzosek, T., & Einarson, A. (2009). Dental care during pregnancy. *Canadian Family Physician*, *55*(6), 598-599.

Zheng Li , Z. L., Yoshita V Holamoge, Waleed Zaid , Michelle L Osborn, Xiaoqian Shan, Shradha Bhatta , Abhirami Jeyaseelan, Yanping Li , Shaomian Yao, and Jian Xu. (Unpublished). *Mouthwash to deliver indocyanine green for near infrared dental fluorescence imaging*.

Zhongqiang Li , Y. V. H., Zheng Li, Jacob T Miller, Michelle L. Osborn, Xiaoqian Shan, Alexandra Ramos, Yanping Li , Waleed Zaid, Shaomian Yao, and Jian Xu. (Unpublished). *Detection and analysis of enamel cracks by ICG-NIRF fluorescence dental imaging and its comparison with dental X-ray*.

VITA

Ms. Yoshita Viraj Holamoge obtained her bachelor's degree in Instrumentation and Control Engineering from Manipal Institute of Technology, Manipal, India. She later joined Louisiana State University to continue her education and to obtain her master's degree. Her focus during her master's academic career was bio-medical imaging. She is anticipated to complete her master's degree in December of 2019.